

Corrosion Studies on Friction Welded Dissimilar Aluminum Alloys of AA7075-T6 and AA6061 –T6

R.Sathish^{1} V.Seshagiri Rao²*

¹Research Scholar, SCSVMV University, Kanchipuram, Tamil Nadu, India.

² Department of Mechanical Engineering, St.Joseph's College of Engineering, Tamil Nadu, India.

*E-mail: sai_27r123@rediffmail.com

Received: 15 February 2014 / Accepted: 22 April 2014 / Published: 19 May 2014

The aim of this work is to study the effects of corrosion behavior on dissimilar friction welded AA7075 and AA6061 both in T6 conditions. The welded samples are initially subjected to tensile test. Based on tensile strength the samples are subjected to potentiodynamic polarization resistance measurements in NaCl solution. It is observed that the parent metal wrought aluminum alloy found to corrode higher than the corresponding friction welded region of joints. Also the corrosion current and the corrosion rate are higher for the AA7075-T6 side compared to the AA6061-T6 side. The minimum and maximum corrosion rate was varied from 1.91 and 5.74 mm/year in different region. Micro structure study was conducted by optical microscopy to validate the results of the weld joints.

Keywords: Friction welding, Tensile strength, Corrosion rate, Optical microscopy.

1. INTRODUCTION

Friction welding is one of the promising technique to join dissimilar aluminum alloys because there is no melting occurs during welding, instead the metals are brought in contact with each other due to this frictional heat is generated and the metal reaches into plastic state and by giving upset pressure weld joints were obtained [1]. Friction welding has represented the superior joint strength when joining dissimilar materials [2]. In recent years non ferrous metal aluminum alloys drawn more attention in application of marine, aerospace and automobile industries due to light weight high strength to weight ratio, together with its natural ageing characteristics. Friction welding process can minimize the formation of the brittle inter metallic compound at the interface because it is carried high pressure, shorter processing time and below melting temperature [3]. The 6061series alloys, silicon-

and magnesium-containing alloys, are present in the ratio required to form magnesium silicide. These alloys have good corrosion resistance and may be inhibited effectively [4].

Weld zone of high strength precipitate alloys such as AA7075 is very high prone to inter granular corrosion on the grain boundaries [5].

The 7075 wrought alloys contain major additions of zinc, along with magnesium or magnesium plus copper in combinations that develop various levels of strength. Those containing copper have the highest strengths and have been used as construction materials, primarily in aircraft applications, for more than 40 years [6].

Among heat-treatable alloys, those of the 6xxx series, which are moderate-strength alloys based on the quasi-binary Al–Mg₂Si (magnesium silicide) system, provide a high resistance to general corrosion equal to or approaching that of non-heat treatable alloys [7].

2. EXPERIMENTAL WORK

Wrought aluminum alloys such as AA6061 and AA7075 both in T6 condition were used in this present work. The chemical composition and mechanical properties of base metal are presented in Table 1 and Table 2. The joints are fabricated by Taguchi L9 orthogonal array at three levels and four parameters as shown in Table 3. Pilot study was conducted to prefer the levels and parameters. The welded samples are initially subjected to drop test and tensile test were carried out according to ASTME E8M-307. Based on the failure, samples were selected for the corrosion test. The selected samples are broken at base metal sample 3 (S3) and high tensile strength sample 9 (S9). For microstructure evaluation inverted metallurgical optical microscopy range 100 -600x was used. For corrosion study potentiodynamic polarization test was conducted as per the standard ASTM G 59-97 on friction welded dissimilar aluminum alloys weld joints. The two welded samples interface junction was compared with the parent metal namely AA6061 & AA7075 –T6 base metal. Saturated calomel electrode was used as reference electrode.

Friction welded sample of 1 cm x 1 cm having the different region namely base metal and the weld zone were cut from the cylindrical specimen in wire EDM processes with the thickness of 1.5mm. In this study a corrosive environment 3.5% of Sodium chloride (weight) was used. The samples are polished by different grades of emery sheets and the impurities were removed.

Table 1. Chemical Composition of base metal AA7075-T6

Elements	Cr	Cu	Fe	Mg	Zn	Al
Wt %	0.22	1.2	0.23	2.1	5.9	Balance

Mechanical Properties of AA7075-T6

Mechanical properties	0.2% Yield strength (MPa)	Ultimate tensile strength (MPa)	Elongation(%)
Values	527	571	12

Table 2. Chemical Composition of base metal A6061-T6

Elements	Si	Cu	Fe	Mn	Mg	Cr	Al
Wt %	0.67	0.31	0.48	0.09	0.99	0.16	Balance

Mechanical properties of AA6061-T6

Mechanical properties	0.2% Yield strength (MPa)	Ultimate tensile strength (MPa)	Elongation (%)
Values	276	306	17.3

Table 3. Different levels of parameters taken for Friction welding

Parameters	Friction pressure (MPa)	Upset pressure (MPa)	Speed of rotation (rpm)	Burn- off length (mm)
Levels				
Level 1	18	22	1000	1
Level 2	22	32	1250	2
Level 3	32	44	1500	3

3. RESULTS AND DISCUSSION

3.1 Tensile test observation

Table 4. Taguchi L9 orthogonal array for Friction welding

Sample No.	Friction pressure (MPa)	Upset pressure (MPa)	Speed of rotation (rpm)	Burn-off length (mm)	Tensile Strength (MPa)
1	18	22	1000	1	81
2	18	32	1250	2	152
3	18	44	1500	3	203
4	22	22	1250	3	189
5	22	32	1500	1	179
6	22	44	1000	2	182
7	32	22	1500	2	212
8	32	32	1000	3	216
9	32	44	1250	1	224

The tensile test were conducted as per ASTME standards as shown in figure. The specimen is loaded in universal testing machine the tensile stress were measured. The materials failed in four

distinct regions namely (i) weld (ii) Thermo-mechanical affected zone (iii) Heat affected zone (iv) Base metal as shown in figure 2(b).

The results of various tensile testing for different combination were estimated. The ultimate tensile strength varies from 81MPa to 224MPa with 13.78% elongation of the strain rate. It is observed that higher upset pressure, friction pressure and lower rotational speed give more tensile strength and more ductility. However, sample 1 is broken at the weld showing a brittle fracture with lower tensile strength of 81MPa, and a low strain rate of 3.41%.

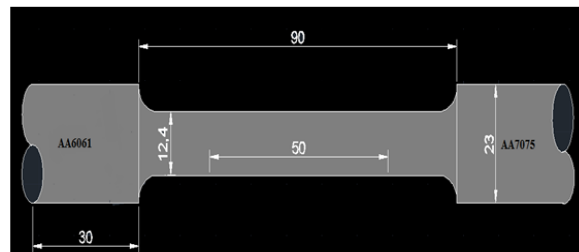


Figure 1. The geometry of tensile test specimen

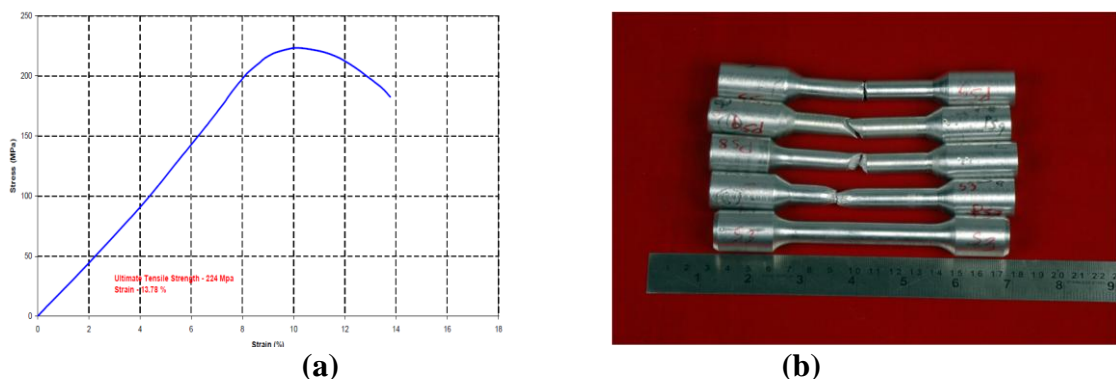


Figure 2 (a) Tensile graph for maximum strength **(b)** Different location of failure

3.2 Corrosion test analysis

David Talbot and James Tabolt [8] studied that passive oxide film can be easily formed on the surface of aluminum alloys when it exposed to air or water it is due to chloride ions. Kenneth R et.al also reveals that presence of chloride ions the corrosion rate is very high and also it depends on heterogeneity of their microstructure [9].

Polarization resistance can be related to the rate of general corrosion for metals at or near their corrosion potential, E_{corr} . Polarization resistance measurements are an accurate and rapid way to measure the general corrosion rate. Electrochemical polarization test methods are extremely pertinent for understanding and evaluating the corrosion resistance of materials and the effect of changes in the corrosive environment. They can establish criteria for anodic or cathodic protection and susceptibility to several forms of corrosion.

Venugopal et. al [10] studied micro-structural and pitting corrosion properties of friction stir weld of AA7075 Al alloy in 3.5%NaCl solution. Corrosion resistance of weld metal is better than that of TMAZ and base metal. Srinivasa Rao and Prasad Rao [11] studied the mechanism of pitting corrosion of heat treatable Al–Cu alloys and welds. In this study, electrochemical corrosion test by Tafel curve extrapolation method was carried out for sample 3 and sample 9. Samples of base alloy AA6061 and AA7075 and friction welded area in sodium chloride solution of 3.5% to determine corrosion parameters such as corrosion potential ($E_{corr.}$) and corrosion current ($I_{corr.}$) as shown in Table 5.

Table 5. Results of corrosion test by potentiodynamic polarization method

Sample I.D.	I_{corr} (Corrosion current in Mamps/cm ²)	Corrosion rate mm/year	Corrosion rate mills/year	Area of the sample Sq centimeter	Rest potential in Mv
S-9	0.1758	1.9147	75.384	1	-783.35
S-3	0.3926	4.2752	168.31	1	-759.6
AA7075	0.5967	5.7453	226.19	1	-733.3
AA6061	0.4207	4.581	180.35	1	-712.94

Generally aluminum alloys, AA7075 are susceptible to galvanic attack near precipitates of MgZn₂ MgAlCu. Srinivasan et.al [12] reported that the general corrosion resistance of the AA6056 parent material is better than the AA7075 parent material due to content of copper. The zinc rich precipitates in the AA7075 alloy causes the formation of micro galvanic cells, leading to higher rates of dissolution. Further, zinc is active when compared to aluminum alloy matrix, hence can enhance the corrosion rate.

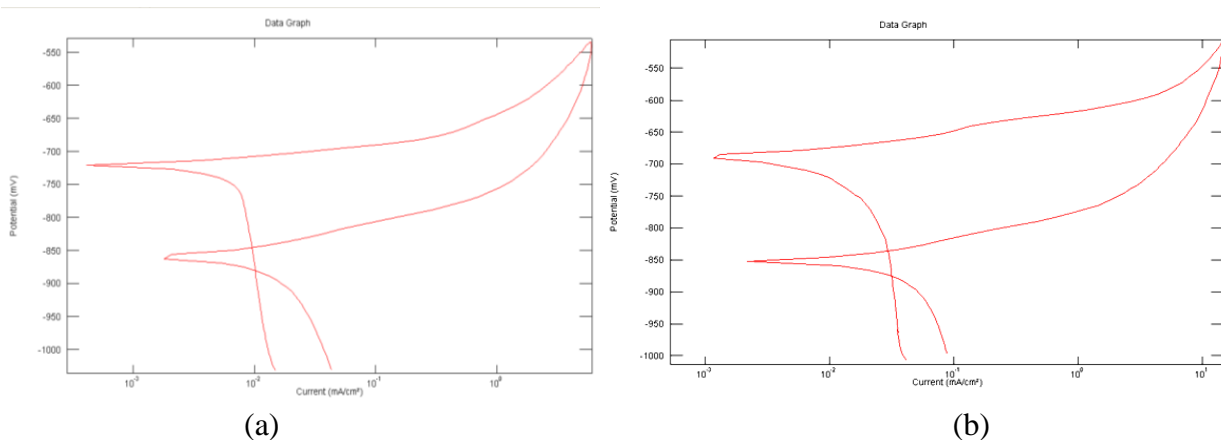


Figure 3. (a) Polarization curve for AA6061 **(b)** Polarization curve for AA7075

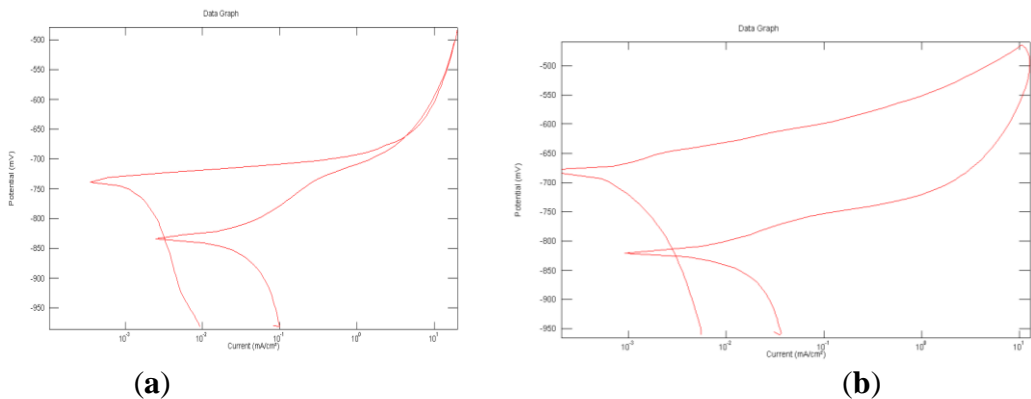


Figure 4. (a) Polarization curve for weld joint (b) Polarization curve for weld joint 9

The sample of polarization curve is shown in figure 3(a & b) at 3.5% NaCl at temperature 29°C. It is observed that the parent metal AA7075-T6 shows high corrosion rate of 5.74 mm per year while AA6061 parent metal imparts 4.27 mm per year and it have better corrosion resistance. Also it is clear that the rest potential is high at weld, thermo mechanically affected zone and heat affected zone wrought aluminum alloy which have high resistance to corrosion than parent metal. This depicts that the rest potential is higher for the parent metal. It is also to be noted that the corrosion current is also higher for the parent metal compared to the welded junction.

For acquiring the Tafel slope by polarization method a cyclic sweep was chosen at the sweep rate of 100 m V. The curve was determined by stepping the rest potential at a scan rate of 0.5mV/sec, from -250 mV to +250 m V vs. SCE. Figure 4(a, b) shows the Tafel plot of weld metals of two samples S3, S9 and reveals the rest potential of -759.6,-783.35 respectively. This result indicate that the sample 3 of the weld joint act as a cathode and give better resistance to corrosion when compared to sample 9.In both the cases the weld metal (core zone) region the metal behaves more corrosion resistance compared to Heat affected zone, thermo mechanical affected zone due to homogeneous distribution of elements present in an aluminum matrix. Linear polarization resistance (LDR ohm cm²) is used to find the measurement of corrosion rate for immediate feedback as well as tendency of pitting. The LDR values of sample 3 and sample 9 is 21.28 and 47.59 ohm cm² respectively. From the data it is clearly indicates that sample 9 has tendency for deep pits and it is validated in micro structural studies.

4. MICROSTRUCTURE

4.1 Parent metal

Optical microscopy study was conducted to the weld samples in parent of AA6061, AA7075 side, weld, HAZ region. The figure 5 (a) shows the microstructure image of potential-dynamic polarization subjected location of AA 7075 wrought alloy surface. The effect of polarization leads to the formation of large corrosion pits. These pits are shown in black color cylindrical shape and occurred severely. In addition the grains boundaries are ditched and nowhere the surface of the metal is

free from corrosion pits. Hence the parent metal of AA7075-T6 is mainly affected by localized corrosion pits.

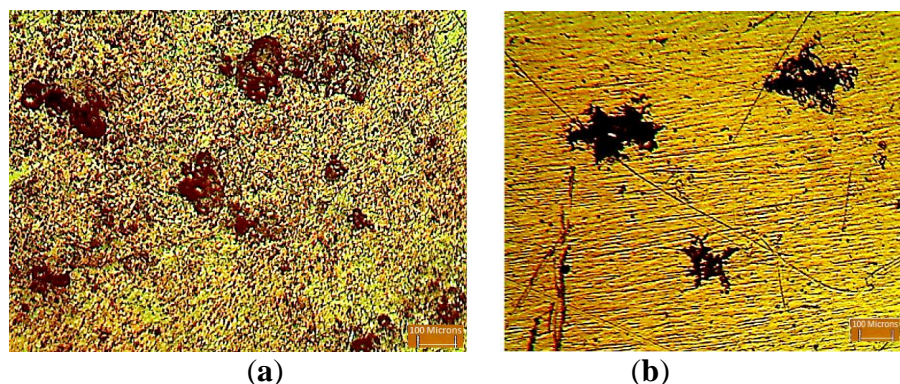


Figure 5. (a) Parent metal AA7075 **(b)** Parent metal AA6061

The Fig. 5 (b) image shows the micro structure of after potential-dynamic polarization subjected to location of AA 6061 wrought alloy surface. The effect of polarization leads to the formation of large corrosion pits formed by the polarization. The pits formed by the potential applied are isolated and majority of the matrix is free from the effect of polarization effects of corrosion.

Sample 3

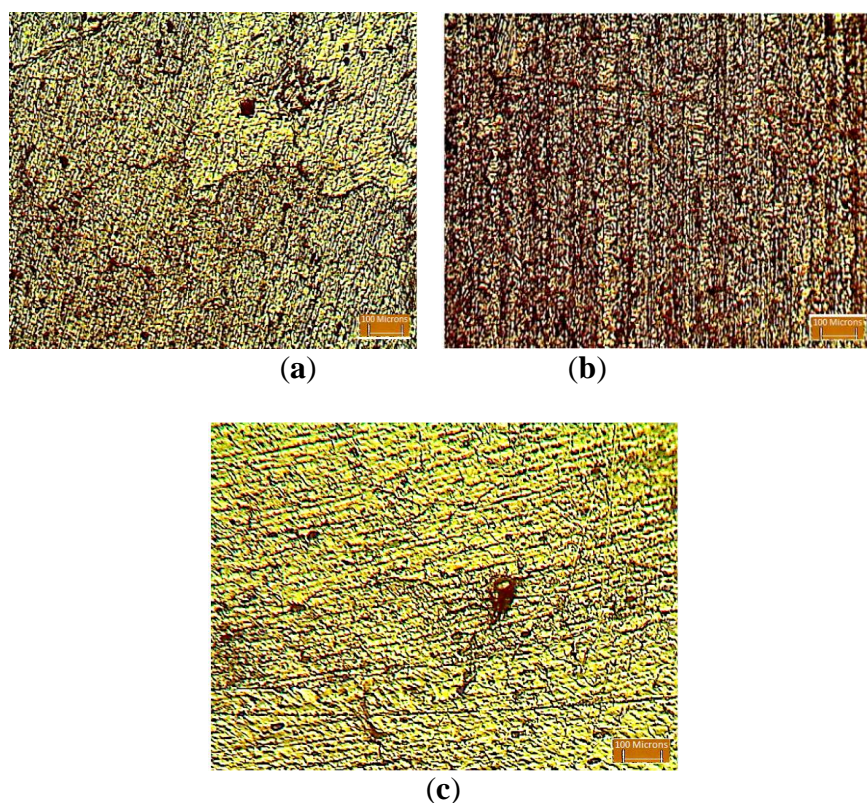


Figure 6. (a) Heat affected zone **(b)** Core zone **(c)** Thermo-mechanical zone (sample 3)

The Fig.6 shows the potential- dynamic polarization of the weld joints of sample (S3 parameters). The effect of polarization leads to the formation of corrosion pits of different gravity. The three corrosion surface images are taken from the fusion zone. Fig. 6 (a) image is taken from the core of the fusion zone which shows better resistant to corrosion but it shows inter granular corrosion by polarization method. G. Elatharasan et.al also reveals that the affected zone of the weld exhibited highest susceptibility to inter-granular corrosion [13]. This zone does not show the presence of deep pits instead, the grain boundaries are marginally ditched. The Fig.6 (b) is taken from the fusion zone which is closer to the AA7075 side. The constituents of the fusion zone are more diluted with 7075 alloy. Hence the corrosion behavior is more and follows the pattern of AA7075. The fig. 6 (c) Shows the fusion zone more diluted with AA6061 and least affected. However the corrosion rate is the consolidated effect of the entire three zones as the corrosion cell covers all the three zones. In S-9 parameter the effect of polarization leads to the formation of corrosion pits of different gravity. The three corrosion surface images are taken from the fusion zone. All the three images shows (Figure 7) severe corrosion pits as well as grain boundary ditches but there is more resistance to corrosion while compare to other zones. It is evident that this surface should have shown more corrosion and the experimental values confirm the same. Moreover fusion zone is more diluted with AA7075 alloy constituents.

Sample 9

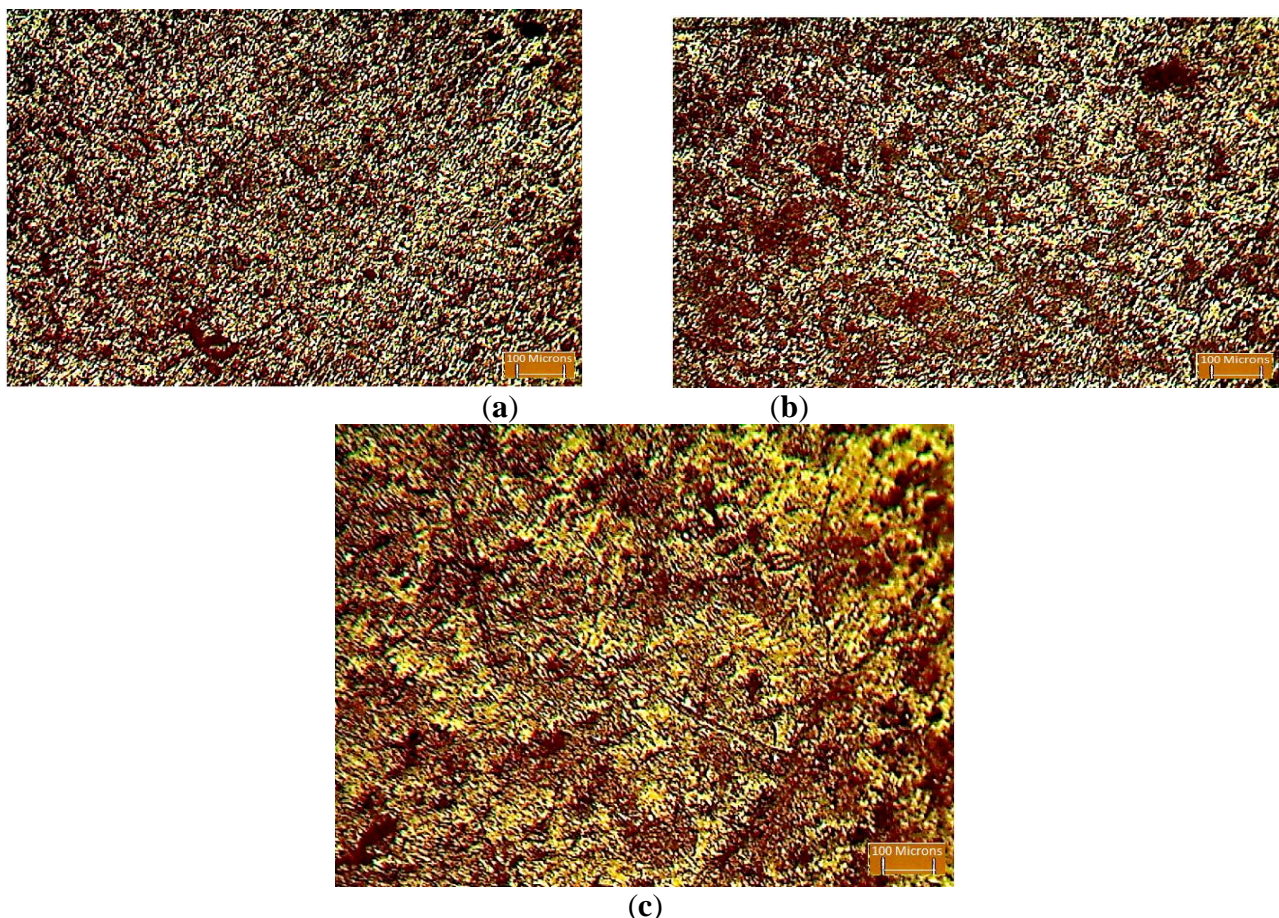


Figure 7. (a) Core zone (b) Heat affected zone (c) Thermo-mechanical zone (sample 9)

5. CONCLUSION

This work investigated effects of friction welded corrosion behavior of dissimilar aluminum alloys. The findings made by the experimental work are given below.

- (1) Two dissimilar aluminum alloys of AA7075 and AA6061 both in T6 condition was joined by friction welding process with a maximum joint strength of 224 MPa was achieved.
- (2) During tensile test the samples were broken at different regions namely weld, HAZ, TMAZ, Parent zone.
- (3) Selected samples are subjected to potentiodynamic polarization test it reveals that the parent metal AA7075 –T6 shows high corrosion rate of 5.74 mm per year while AA6061 parent metal imparts 4.27 mm per year and it have better corrosion resistance.
- (4) The corrosion rate is less in both the samples at weld zone when compared to parent zone.
- (5) The rest potential is high at weld, thermo mechanically affected zone and heat affected zone wrought aluminum alloy which have high resistance to corrosion than parent metal.
- (6) Microstructure of parent metal AA7075 side shows the grains boundaries are ditched and nowhere the surface of the metal is free from corrosion pits. Micro structure of parent metal AA6061 side, majority of the matrix is free from the effect of polarization effects of corrosion.
- (7) Microstructure of sample 3 in fusion zone shows better resistant to corrosion but it shows inter granular corrosion by polarization method. This zone does not show the presence of deep pits instead, the grain boundaries are marginally ditched.
- (8) Microstructure of sample 9 shows the formation of pits in different gravity and the fusion zone is more diluted by AA7075 constituents.

ACKNOWLEDGEMENT

The authors express their gratitude to SCSVMV University, Kanchipuram and St. Joseph's College of Engineering, Chennai. The authors are thankful to Mr. Rangan from IIT, Madras for their constant encouragement while carrying out this work.

References

1. B. S. Yilbas, A. Z. Sahin, N. Kahraman and A. Z. Al-Garni: *J. Mater. Process. Technol.*, 49 (1995) 431 – 443
2. W. B. Lee, Y.M. Yenon, D.U.Kim, S.B.Jung, *Material Science Technology*, 19 (2003) 773-778.
3. Won-BaeLee, Kuek –Saeng Bang, Seung-Boo Jung *Journal of Alloys and compounds*, 390 (2005) 212-219.
4. B.W. Lifka, Corrosion Engineering Handbook, edited by P. A. Schweitzer. Marcel Dekker, New York. (1996) 99–106.
5. J.B. Lumsden, M.W. Mahoney, G. Pollock, C.G. Rhodes, *Corrosion* 55 (12) (1999) 1127.
6. J. G. Kaufman and E. L. Rooy, Corrosion Test and Standards, Application and Interpretation, 2nd edition, edited by R. Baboian. ASM International, Materials Park, OH, (2005) 1–8.

7. J. G. Kaufman, in ASM Handbook, Volume 13B, Corrosion: Materials, edited by S. D. Cramer and B. S. Covino Jr. ASM International, Materials Park, OH, (2005) 95–124.
8. David Talbot and James Talbot, *Corrosion Science and Technology*, CRC Press LLC, 1998.
9. R. Kenneth, Trethewey and J. Chamberlain, *Corrosion for Science and Engineering*, Longman Group Limited, 2nd Edition, 1996.
10. T. Venugopal, K. Srinivasa Rao, and K. Prasad Rao, *Trans. Indian Inst. Metals*, 57 (2004) 659-663.
11. K. Srinivasa Rao, and K. Prasad Rao, *Transaction of Indian Institute of Metals*, 57 (2004) 503-610.
12. P.B. Srinivasan, W. Dietzel, R. Zettler, J. dos Santos, V. Sivan, *Corrosion Engineering Science and Technology* 42 (2007) 161-167
13. G.Elatharasan and V.S.Senthil Kumar, *Journal of Mechanical Engineering*, 60 (2014) 29.

© 2014 The Authors. Published by ESG (www.electrochemsci.org). This article is an open access article distributed under the terms and conditions of the Creative Commons Attribution license (<http://creativecommons.org/licenses/by/4.0/>).